

## ELECTROCHEMICAL IMPEDANCE SPECTROSCOPY IN NITRATE SOLUTIONS CONTAINING MONOSODIUM GLUTAMATE USING SCREEN-PRINTED ELECTRODES

Dora Domnica BACIU<sup>1</sup><sup>1</sup>, Andreea MATEI<sup>2</sup>, Anca COJOCARU<sup>3\*</sup>,  
Teodor VISAN<sup>4</sup>

*Electrochemical impedance spectroscopy technique has been used to characterize commercial screen-printed electrodes (SPEs) in monosodium glutamate (MSG) aqueous solutions at open-circuit potential and room temperature. Additionally, considerations have been made about the chemical nature of existing species (undissociated MSG molecules, glutamate ions and zwitterions) and have processed the conductivity data from literature by calculating and selecting specific conductivity for diluted MSG solutions, 0.5 M  $KNO_3$  and 0.5 M  $NaNO_3$ . In first experiments, SPEs based on Au, Pt and carbon (graphite) materials were studied in 1 mM MSG dissolved in deionized water. Nyquist and Bode spectra were comparatively recorded only on gold SPEs in 100  $\mu M$  and 1 mM MSG solutions having 0.5 M nitrate salts ( $KNO_3$  or  $NaNO_3$ ) as supporting electrolyte. In addition to the capacitive behavior, inductive loops attributed to competitive adsorption between glutamate species and nitrate ions were highlighted. Fitting of experimental data with three equivalent circuits as models has allowed the evaluation of impedance parameters related to charge transfer rate, double layer capacity and adsorption components (resistance, inductance, and capacitance).*

**Keywords:** Monosodium glutamate, nitrate ions, electrochemical impedance spectroscopy, screen-printed electrodes, adsorption

### 1. Introduction

Sodium salts of L-glutamic acid may be monosodium glutamate (MSG) and disodic glutamate. MSG is the most known taste and flavour enhancer, which promotes the sensory perception of the meat-like aroma (*umami* flavour), thus

<sup>1</sup> PhD student, Depart. of Inorganic Chemistry, Physical Chemistry & Electrochemistry, University POLITEHNICA of Bucharest, Romania, e-mail: popescudomnica@yahoo.com

<sup>2</sup> Senior researcher 1<sup>st</sup> degree, PhD, National Institute for Laser, Plasma & Radiation Physics (INFLPR), Magurele, Ilfov county, Romania

<sup>3\*</sup> Prof., Depart. of Inorganic Chemistry, Physical Chemistry & Electrochemistry, University POLITEHNICA of Bucharest, Romania, e-mail: anca.cojocaru@chimie.upb.ro

<sup>4</sup> Emeritus Prof., Depart. of Inorganic Chemistry, Physical Chemistry & Electrochemistry, University POLITEHNICA of Bucharest, Romania

influencing food choice. According to European Union classification, MSG has the HS code 29224220 and E-621 number. When added to foods or in solutions, MSG dissociates predominantly as glutamate monovalent anion. Both the naturally-occurring glutamate ionic species and the one derived from MSG dissociation are chemically indistinguishable and human bodies metabolize them in the same way. L-glutamate is also an excitatory neurotransmitter in the central nervous system of organism. There is a continuing and growing need for electrochemical detection of glutamate and the published results are covered by many reviews, some recent being refs. [1-5]. Almost all sensors are based on enzymatic activity and hold significant attention because of their reasonable limit of detection, reliability, affordability and ease of handling. Non-enzymatic sensors developed for the detection of glutamate using different electrode materials as gold [4], carbon modified with gold [5] and nickel nanowire array or this array modified with Pt [6,7]. However, it was noticed that non-enzymatic biosensors had poor selectivity for the detection of the low level of L-glutamate concentration ( $\mu\text{M}$ ), therefore not suitable for field applications.

Screen printed electrodes (SPEs) are considered be the most appropriate electrochemical sensors for in situ analysis because of their linear output, low power requirement, quick response, high sensitivity and ability to operate at room temperature. Many commercial sources of SPEs in different configurations exist for glutamate sensing [8-10], although in many cases the authors used 'home made' SPEs by printing different inks on electrode material. SPEs present several advantages versus conventional electrodes as they are appropriate for working with low volumes of sample (low consumption of reagents) and permit the development of sensitive, accurate and reproducible sensors.

In modern devices, the multisensor arrays called 'electronic tongue' were used to detect analytes at ultratrace level in glutamate samples [11,12]. These devices exhibit various selectivity and pattern recognition systems that analyze the sensor responses, thus being dedicated to automatic chemical analysis of samples and recognition of their characteristic properties. In impedentiometric mode of operation, the procedure is based on the measurement of impedance or capacitance changes either at one fixed *ac* frequency or a broader spectrum using impedance spectroscopy. Electrochemical impedance spectroscopy (EIS), as a non-destructive and sensitive technique, is important to study the intrinsic ohmic resistance of solution and the resistance of charge transfer as well as electrolyte ions diffusion and corrosion processes [13-17]. The impedance measurement is advantageous because of the experimental simplicity and better performance for detection of organic substances, such as glutamate species. In this work we present investigations regarding impedance characteristics of screen-printed electrode / MSG solution interface. For the purpose of better electrochemical sensing of monosodium glutamate in diluted solutions we chose alkali metal

nitrates as supporting electrolytes to enhance conductivity of solution. Surface characteristics of commercial three screen-printed DropSens electrodes (Au, Pt and carbon) and electrochemical activity (electron transfer) of glutamate neutral or ionic species are characterized by electrochemical impedance spectroscopy.

## 2. Experimental

### 2.1. Materials and Instruments

All reagents used (monosodium glutamate monohydrate (>99%), potassium nitrate and sodium nitrate) were of analytical grade and were purchased from Merck-Millipore. Deionized ultrapure water (AD) was obtained from a TKA GenPure system with a TKA Pacific UP / UPW6 sterile filter. Supporting solutions 0.5 M  $\text{KNO}_3$  and 0.5 M  $\text{NaNO}_3$  were prepared in calibrated volumetric flasks. The prepared concentrations of MSG dissolved in AD or in supporting solutions were 100  $\mu\text{M}$  and 1 mM and pH was adjusted to 9.38.

Screen printed electrodes (SPEs) were purchased from Metrohm DropSens [18]. Method of screen printing allows one to construct the whole electrode system on strips based on alumina ceramic substrate with 33 mm  $\times$  10 mm  $\times$  0.5 mm size. A three-electrode configuration was painted (printed) by manufacturing company with different inks on their surface and an insulating layer served to delimit the electrode areas (working, auxiliary and reference electrodes) from silver electrical contacts. The working electrodes, each having 4 mm diameter ( $0.1256 \text{ cm}^2$ ), were gold (DRP-220AT), platinum (DRP-559) and carbon (graphite, DRP-110). The auxiliary electrodes were also made of Au, Pt and C, respectively, while the reference electrodes were of Ag in all cases. The use of special cable connector (ref. CAC, DropSens) allowed a connection of SPE to Autolab PGSTAT 302N potentiostat provided with impedance phase analyzer, which runs with NOVA 2.0 software.

### 2.2. Method

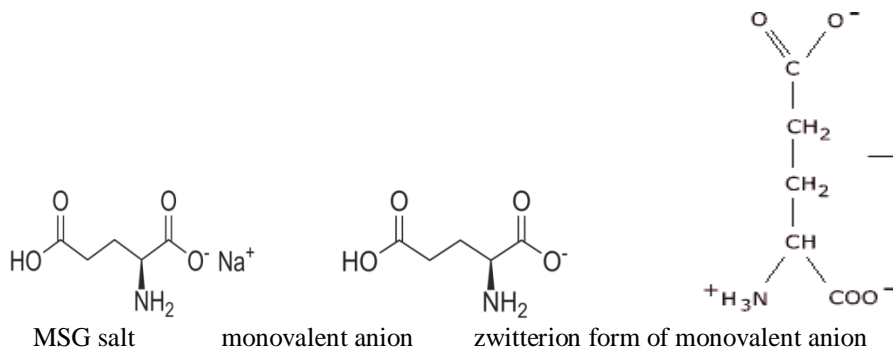
EIS measurements were made at room temperature by applying a sinusoidal waveform voltage (*ac* signals) with 10 mV amplitude, over a frequency range within 100 kHz and 100 mHz. Before each EIS test, the samples were kept in the 10 mL MSG solution for 30 minutes to stabilize the open-circuit potential of SPEs. The impedances were represented as Nyquist (imaginary part of impedance  $Z_{\text{Im}}$  *vs.* real part  $Z_{\text{Re}}$ ) and Bode (phase angle and impedance modulus  $/Z/$  *vs.* frequency) diagrams. The plots were analyzed and fitted with equivalent electrical circuits by using ZView 2.4 software from Scribner Assoc. Inc., Derek Johnson.

### 3. Results and discussion

#### 3.1. Some considerations about electrical conductance of MSG solutions

Monosodium glutamate is a 1:1 type electrolyte because in its first dissociation step both  $\text{Na}^+$  and monovalent glutamate anion result. It also behaves as a non-associated electrolyte [19].

The next dissociation step of anion produces  $\text{H}^+$  and divalent glutamate anion. Values of the equilibrium constants of both dissociation processes are known in the literature showing that sodium glutamate dissolved in water behaves as a strong electrolyte, i.e. is almost totally dissociated. However, the problem is more complex because the basic amino groups in monovalent glutamate anion can be protonated and simultaneously the carboxylic acidic groups deprotonated, therefore the monovalent glutamate changes its structure as zwitterion species. Thus, an aqueous solution of MSG mostly contains different proportions of sodium, hydrogen cations and glutamate anions, but also undissociated MSG molecules and dipolar glutamate ions as zwitterions (Scheme 1).



**Scheme 1** Some of the main chemical species as constituents in MSG aqueous solutions

It is known that a low conductivity of the electrolyte limits the use of cyclic voltammetry or other electrochemical techniques by adding a parasitic ohmic polarization (ohmic drop) in series with the faradaic overvoltage. This is also the case of ionic conductance in MSG diluted solutions. In [20], systematic measurements about electrical conductivity of dilute aqueous MSG solutions at various temperatures were reported. Values of equivalent (molar) conductivity at 298.15 K lie in the range from 80.27 and 74.27  $\text{S cm}^2 \text{ mol}^{-1}$  for concentration domain of 0.25 mM to 5.07 mM MSG, respectively. We have processed the experimental data of limiting equivalent conductivities from this work by calculating specific conductivity ( $\lambda$ ) for each concentration of MSG at room temperature. The values are listed in Table 1. Indeed, it can be seen that electrical conductivity  $\lambda$  is very low to the most diluted solution, it slightly increases with

concentration of MSG and is expected to reach useful values only for relatively concentrated solutions (solubility of MSG in water being 740 g/L).

*Table 1*  
Recalculated values of specific conductivity using data from [20]

MSG concentration (mM)	$\lambda$ at 298.15 K (mS cm <sup>-1</sup> )
0.250	0.200
0.510	0.401
0.760	0.600
1.010	0.792
2.530	1.929
5.070	3.765

However, for practical applications of sensors which analyze MSG extracts from food samples, for instance, values of 1-5 mS cm<sup>-1</sup> conductivity are still too low and therefore the conduction of solution should be improved. We opted to add alkali metal nitrate salts such as KNO<sub>3</sub> or NaNO<sub>3</sub> which by dissolving in water will play the role of supporting electrolyte in our measurements. Solubility of alkali metal nitrates in water is very high and specific conductance of their aqueous solutions can be taken from the usual Tables of physical properties. Values of 47.0 mS cm<sup>-1</sup> [21] and 46.2 S cm<sup>-1</sup> [21-23] were selected for 0.5 M KNO<sub>3</sub> solution and 0.5 M NaNO<sub>3</sub> solution, respectively. It is obvious that adding MSG concentrations between 0.1 mM and 3 mM in a 0.5 M nitrate solution cannot drastically change the ionic conductance of electrolyte. Taking into account the screen-printed electrode surface area (0.1256 cm<sup>2</sup>) and distance of working electrode to the other integrated electrodes (counter and reference) of almost a millimeter on each SPE strip, the ohmic resistance of the solution is expected to be of the order of one thousand ohms or less. These calculated conductivity results can hardly be compared with data in the literature since measurements with screen-printed electrodes in glutamate solutions have not been reported until now.

### 3.2. EIS characterization of screen-printed electrode / MSG solution interface

The electrochemical impedance spectroscopy (EIS) is a well-known method to determine the electrochemical behavior of the electrode/electrolyte interface. Screen-printed electrodes (SPEs) represent a possible development direction for sensors to be used for routine analysis. However, according to our best knowledge no EIS measurements in monosodium glutamate solutions have been reported so far. Nevertheless, some related EIS studies were carried out

regarding glutamic acid adsorption onto metallic surface (Al [24] or Cu-Ni alloy [25]) in investigations to use this amino acid as corrosion inhibitor.

In this section we examine the main impedance behavior of commercial SPEs as electrodes in aqueous solutions of monosodium glutamate. The MSG solution is an ionic conductor and the electrical conduction process is described in recorded EIS plots by ohmic resistance of solution  $R_s$ . The working with small surface SPEs leads to high  $R_s$  resistance, as shown above; this electrolyte resistance is located at the equipotential interface between the reference electrode and working electrode.

Typical impedance spectra recorded at steady state (open circuit) potential for gold, platinum and carbon SPEs from DropSens in simple MSG solutions (where monosodium glutamate was dissolved in deionized water AD) are depicted in Figs. 1-3. As a general remark, all three kinds of screen-printed electrodes exhibited typical *ac* impedance characteristics of an electrode surface where the attached molecules or ionic species from solution cannot form a firm adsorbed film.

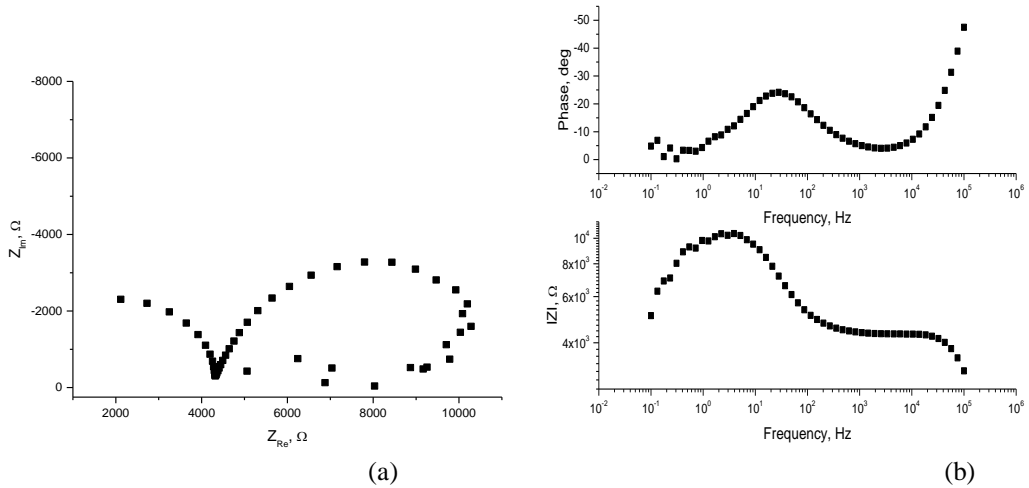


Fig. 1 Nyquist spectra (a) and Bode spectra (b) spectra on Au electrode for 1 mM MSG solution without adding support electrolyte

The Nyquist spectrum on Au electrode (Fig. 1a) shows first a semicircle arch up to  $4200 \Omega$  (i.e. intersection with Ox axis), a value that includes the ionic resistance of electrolyte  $R_s$  together with intrinsic electrical resistance of electrode material and contact resistance between gold electrode and current collector. It should be noted that the biggest contribution is probably made by bad electrical contact, because Au metal must have a good conduction and the solution may have maximum hundreds or one thousand ohms, as seen above. However, we observed experimentally that this complex resistance increased by an order of magnitude for more diluted solution, i.e.  $100 \mu\text{M}$  MSG in water (its impedance

plots not shown here), a fact that suggests poor conduction for very diluted solutions. The Nyquist plot continues with a capacitive semicircle with a larger diameter representing the charge-transfer resistance  $R_{ct}$ ; its value of more around  $7500\ \Omega$  is related to the charge transfer limitation at the electrode/electrolyte interface. Bode diagram (Fig. 1b) shows a maximum phase angle of  $-25^\circ$  (at a frequency of 20-30 Hz) which is far from the value of a perfect capacitor (max.  $-90^\circ$ ).

The Nyquist semicircle is followed by a weakly inductive return that is a loop in which the imaginary component of the impedance  $Z_{Im}$  has low but still negative values. This behavior is indicative of a weak adsorption of MSG molecules or electroactive ionic species (glutamate anion, zwitterion form). In Bode plots, the phase angle decreases up to zero at lowest frequency and impedance modulus  $|Z|$  increases linearly with a slope close to 1 with decreasing frequency starting from 100 Hz; however, it finally decreases.

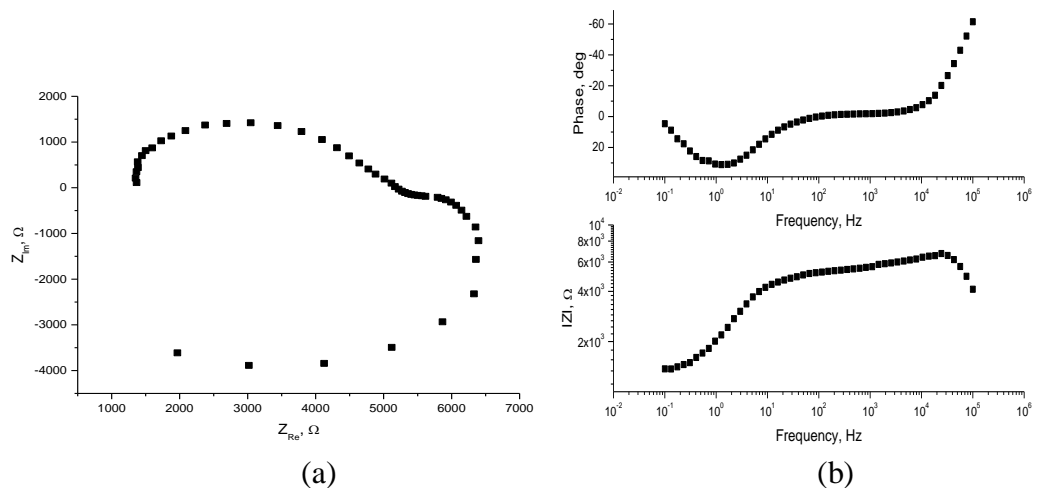


Fig. 2 Nyquist (a) and Bode (b) spectra on Pt electrode for 1 mM MSG solution without adding support electrolyte

Fig. 2 shows at high frequencies on Pt electrode a direct occurrence of a flattened charge transfer semicircle which starts from an interception with X-axis of about  $1250\ \Omega$ ; of course, this value of resistance includes mainly the ohmic resistance of the electrolyte whereas the other components may be negligible. The diameter of capacitive semicircle ( $R_{ct}$ ) is around  $4500\ \Omega$  and its depressed shape may be explained by porosity and uneven surface of platinum electrode. The phase angle decreases with frequency to a value near to 0. In the area of intermediate frequencies the Nyquist curve has a short horizontal portion, while the phase angle remains constant at zero due a good electrical conduction of uncovered metallic surface; the Bode impedance modulus has a linear very small

decrease. Similar to Au electrode, Nyquist curve on Pt at low frequencies continues with a return through a clearly inductive semicircle loop but having much positive values of imaginary part of impedance. This curving of the back plots toward the real axis also indicates that the impedance at long times was limited by adsorption of MSG or glutamate species. Correspondingly, in Bode diagram the second maximum phase angle reaches a positive value, around  $+30^\circ$  at 1 Hz, whereas the impedance modulus decreases by an order of magnitude at its lowest value.

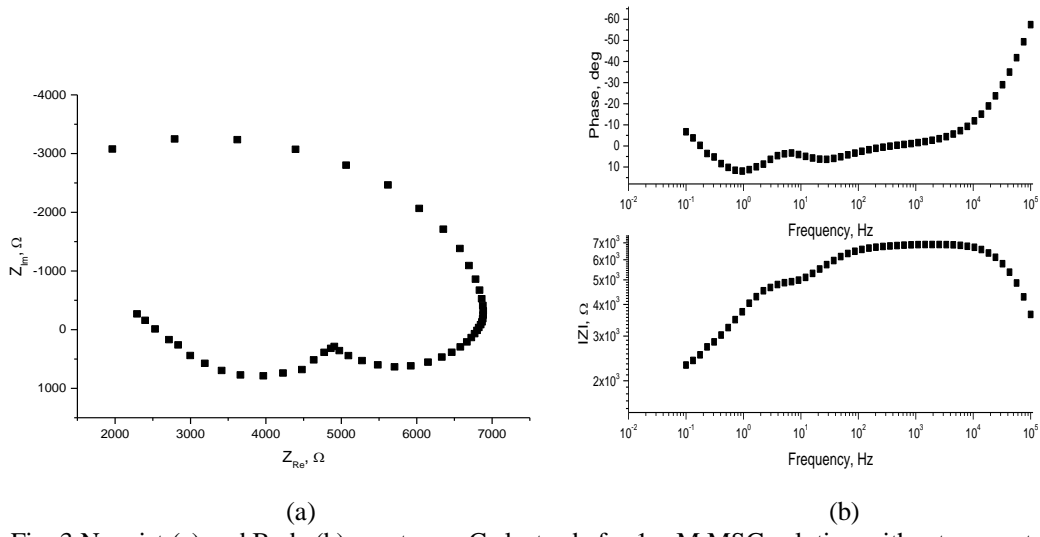


Fig. 3 Nyquist (a) and Bode (b) spectra on C electrode for 1 mM MSG solution without support

Nyquist plot for carbon SPE (Fig. 3a) shows clearly one broader high frequency capacitance loop followed in return by a sequence of one medium frequency inductive loop and one low frequency inductive loop. Although it is not drawn, it seems that the ohmic resistance at the beginning consists mainly in ionic resistance of solution with a value of 500-1000  $\Omega$ . Certainly, the capacitance loop magnitude ( $R_{ct}$ ) of around 6000  $\Omega$  or a little more is determined by the barrier performance of the electric double layer between C electrode and MSG solution. We notice that  $R_{ct}$  value is similar or close to the behavior of the Au and Pt electrodes and this result suggests a slow electron transfer to the glutamate ionic species which is quite little electrochemically active in solutions without a supporting electrolyte. In Fig. 3b the plot of phase angle shows a decrease to zero and two positive maxima, first of  $+7^\circ$  (at 30 Hz) and second much higher maximum of  $+11^\circ$  (at 1 Hz). Bode impedance modulus curve exhibits an increase of  $|Z|$  followed by two plateaus and a final decrease at lowest frequencies. Two inductive maxima and two plateaus of  $|Z|$  suggest two consecutive steps of adsorption due to instable attached species that leave free the electrode surface.

EIS analysis was also carried out to examine the main behavior of Au screen printed electrodes in aqueous solutions of glutamate containing additions of  $\text{KNO}_3$  or  $\text{NaNO}_3$  as supporting electrolyte. For this, gold electrodes with good contact at the current collector were carefully selected and it was chosen a sufficiently high concentration (0.5 M) of nitrate salts. It is expected for the Au electrode to have a better catalytic electroactivity than the other electrodes [4,5]. Typical impedance spectra are depicted in Figs. 4-9.

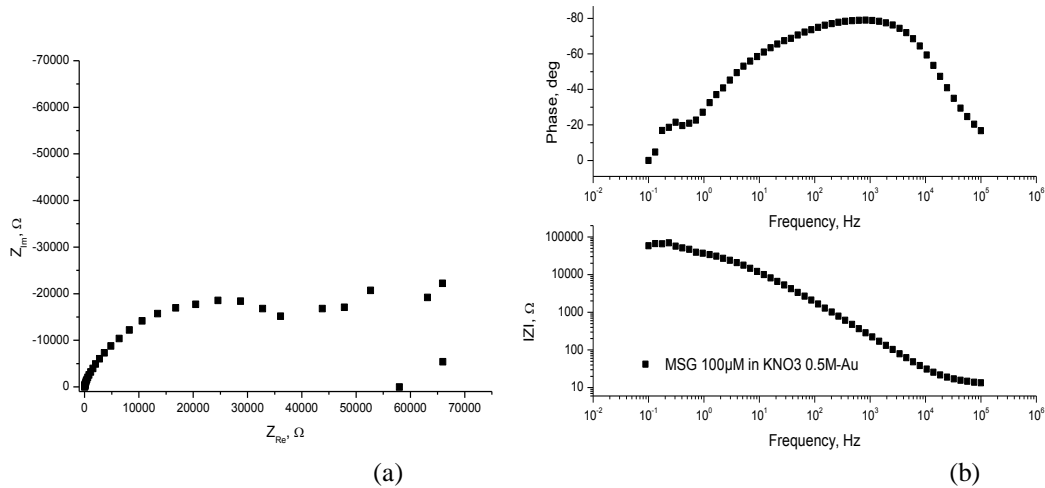


Fig. 4 Nyquist (a) and Bode (b) spectra on Au electrode for  $100 \mu\text{M}$  MSG +  $0.5 \text{ M}$   $\text{KNO}_3$  solution

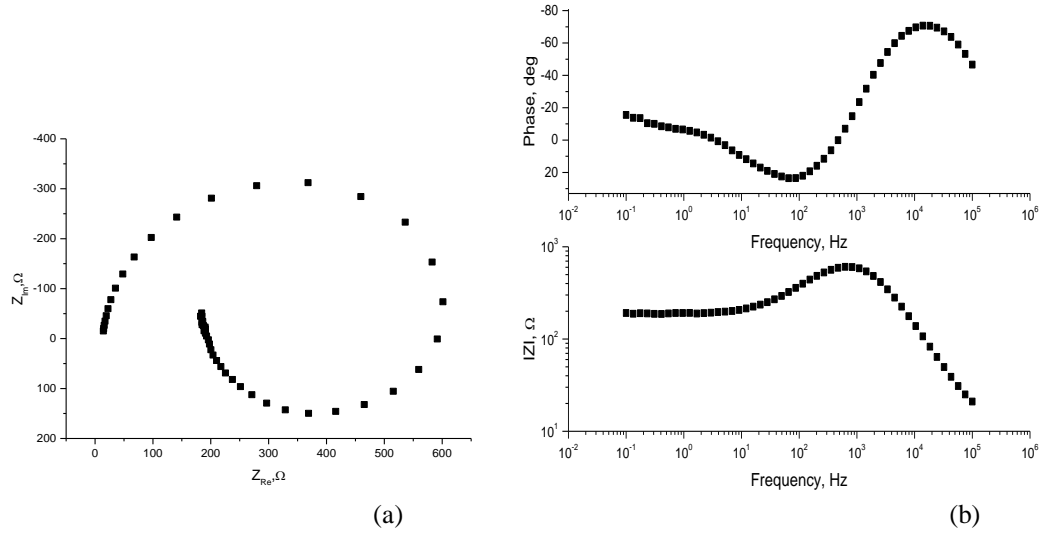


Fig. 5 Nyquist (a) and Bode (b) spectra on Au electrode for  $1 \text{ mM}$  MSG +  $0.5 \text{ M}$   $\text{KNO}_3$  solution

Fig. 4a demonstrates the favorable influence of the supporting electrolyte (potassium nitrate) on the conduction of  $100 \mu\text{M}$  MSG +  $0.5 \text{ M}$   $\text{KNO}_3$  solution because Nyquist curve starts from an ohmic resistance of only few ohms. A single

nondepressed capacitive semicircle appears and the diameter value of several tens kohms is found similar as for 100  $\mu$ M MSG solution without the potassium salt (Fig. 6). The huge value of  $R_{ct}$  proves again a slow charge transfer in electrochemical processes, specific to diluted solutions in glutamate species. The maximum phase angle of  $-80^\circ$  at 100 Hz (Fig. 4b) corresponds to a near perfect capacitor meaning that almost no faradaic processes occur. Probably many  $\text{NO}_3^-$  ions preferentially accumulate close to the gold electrode, and these ions also attract opposite charged ions ( $\text{H}^+$ ,  $\text{Na}^+$ ) to form a double layer thus repelling glutamate species. This is confirmed by several experimental points arranged on a straight line following the Nyquist semicircle in Fig. 4a. Due to the instability, the layer falls apart leading to the last points in returning Nyquist plot. Correspondingly, the phase angle in Fig. 4b has a horizontal limitation at  $-20^\circ$  (at 0.5-1 Hz) which means adsorption/desorption of attached species leaving intermittently the electrode surface free. The impedance modulus increased linear almost over the entire frequency range.

The EIS for 1 mM MSG + 0.5 M  $\text{KNO}_3$  solution spectra change dramatically proving an increased electrochemical activity of glutamate species, quite uninhibited by the presence of nitrate ions. The increased concentration of MSG led to the appearance of a single Nyquist semicircle that is purely capacitive and nondepressed (Fig. 5a). Its diameter of approx. 600  $\Omega$  means a lower  $R_{ct}$  value by an order of magnitude compared to  $R_{ct}$  for 100  $\mu$ M MSG + 0.5 M  $\text{KNO}_3$  (Fig. 4a), as well as compared to  $R_{ct}$  for 1 mM MSG dissolved in water without electrolyte support (Fig. 1a). Fig. 5b shows a maximum phase angle of  $-70^\circ$  (at 2 kHz), just characteristic of non-ideal capacitor (quasi-capacitor). At low frequencies the return loop on Nyquist curve is a clear inductive semicircle (i.e. positive values of imaginary component of impedance) due to the adsorption / desorption equilibrium of MSG species which are predominantly attached; this process was noticed on other metallic electrodes [25]. It is well known that intrusion of organic molecules, such as glutamate species, into the electrochemical double layer ( $dl$ ) changes both its composition and its structure because their presence may decrease the effective dielectric constant and possibly increases  $dl$  thickness [24]. Bode curve exhibits in this frequency region a second maximum angle but having positive value of  $+20^\circ$  (at 100 Hz).

Fig. 6 presents comparatively Nyquist and Bode spectra for the above discussed systems with  $\text{KNO}_3$  addition, where differences in behavior of gold electrode are highlighted. It clear be seen the increase in charge transfer to more concentrated MSG solutions, the most intense being for 1 mM MSG + 0.5 M  $\text{KNO}_3$ , where the diameter of the Nyquist semicircle is the smallest (Fig. 6a,b). Also, Bode-angle plot shows a gradual decrease of the phase angle maximum as well as its shift to lower frequency (Fig. 6c). In the last Fig. there is also a gradual

decrease by an order of magnitude of the impedance modulus in approximately the same order as for the maximum phase angle.

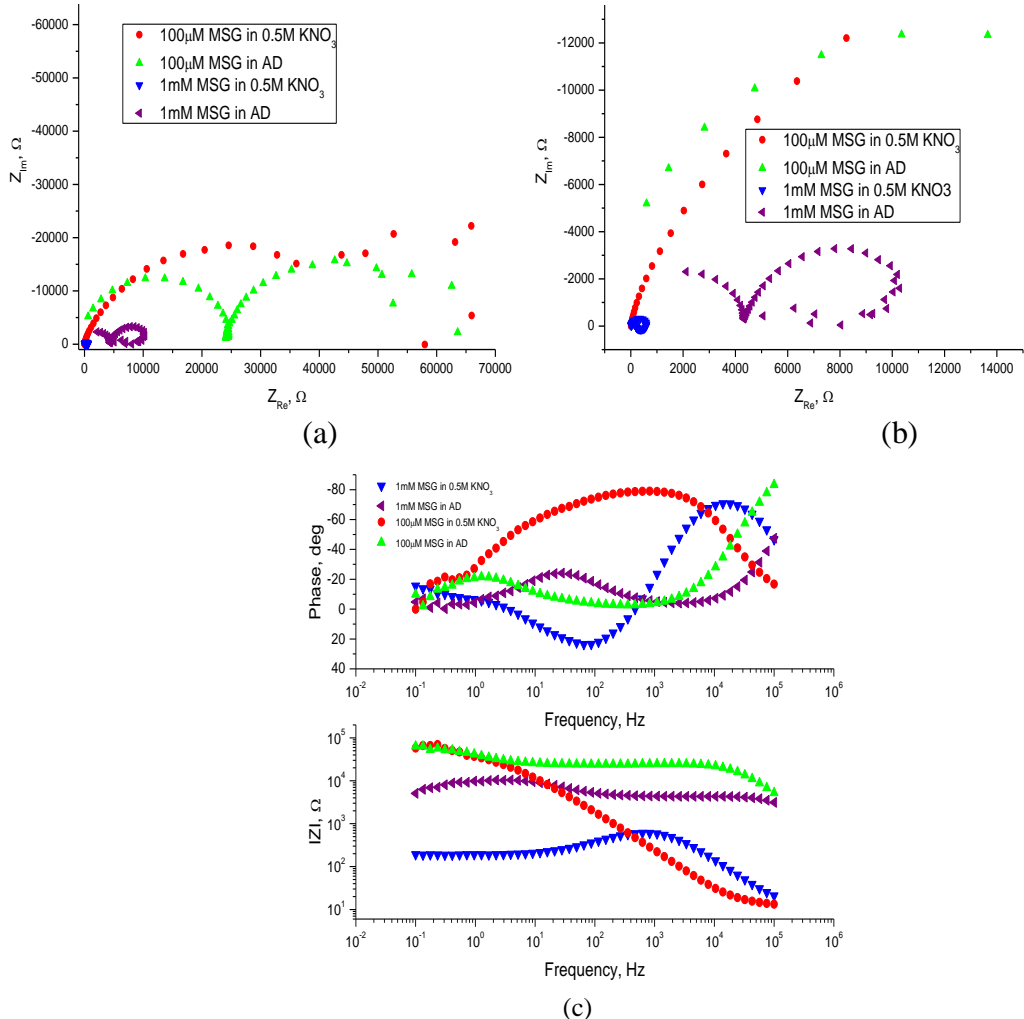


Fig. 6 Nyquist (a,b) spectra and Bode spectra (c) on Au electrode for  $100\text{ }\mu\text{M}$  and  $1\text{ mM}$  MSG solutions without (AD) and with  $0.5\text{ M KNO}_3$  supporting electrolyte

We present in Figs. 7-9 the results obtained by similar impedance studies for the same MSG aqueous solutions when the added supporting electrolyte was  $\text{NaNO}_3$ . Unexpectedly, some differences in EIS behavior were found.

First, there are identical shapes of Nyquist spectra for both  $100\text{ }\mu\text{M}$  and  $1\text{ mM}$  MSG systems with  $0.5\text{ M NaNO}_3$ , which are different from the shapes in solutions with  $\text{KNO}_3$  support. Both Figs. 7a and 8a exhibit a single capacitive semicircle continued with a horizontal straight line as inductive returning to small or even zero values of imaginary impedance. The decrease in semicircle diameter

from  $6500 \Omega$  for diluted  $100 \mu\text{M}$  solution to  $4300 \Omega$  for concentrated  $1 \text{ mM}$  solution is not an order of magnitude smaller, as is expected and as is the case with  $\text{KNO}_3$  addition. Also, the horizontal return of Nyquist curve can mean a very poor adsorption of the species from the solution, as opposed to the intensification of this process in systems with  $\text{KNO}_3$  (Fig. 5a). An explanation may be that the proportion of attached nitrate ions on Au electrode is higher in these solutions with  $\text{NaNO}_3$  support than with  $\text{KNO}_3$ .

Secondly, although the phase angle maxima in Figs. 7b and 8b have about the same value ( $-74^\circ$  and  $-78^\circ$ ) indicating a non-ideal capacitor behavior, they are recorded at much higher frequencies of *ac* voltage (1 and 6 kHz) compared to the frequencies (0.1 and 2 kHz) in  $\text{KNO}_3$  systems.

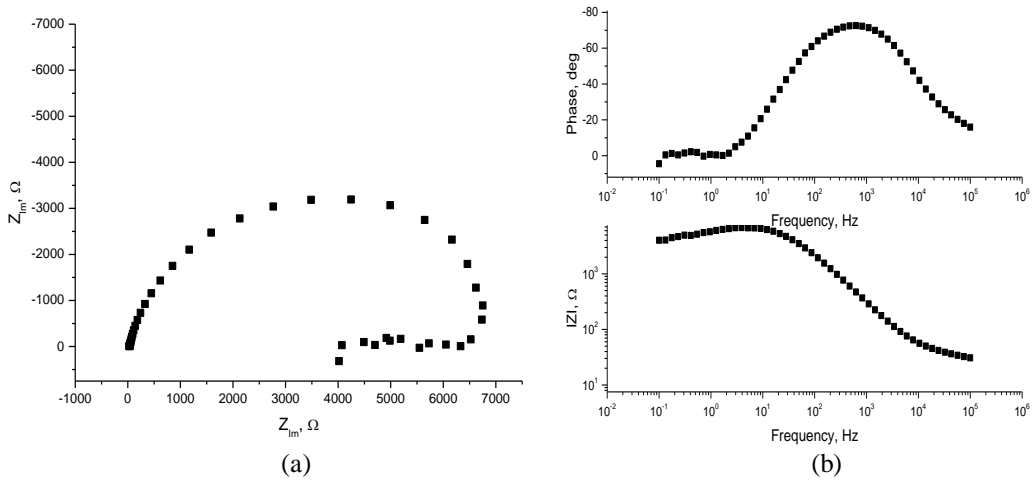


Fig. 7 Nyquist (a) and Bode (b) spectra on Au electrode for  $100 \mu\text{M}$  MSG +  $0.5 \text{ M}$   $\text{NaNO}_3$  solution

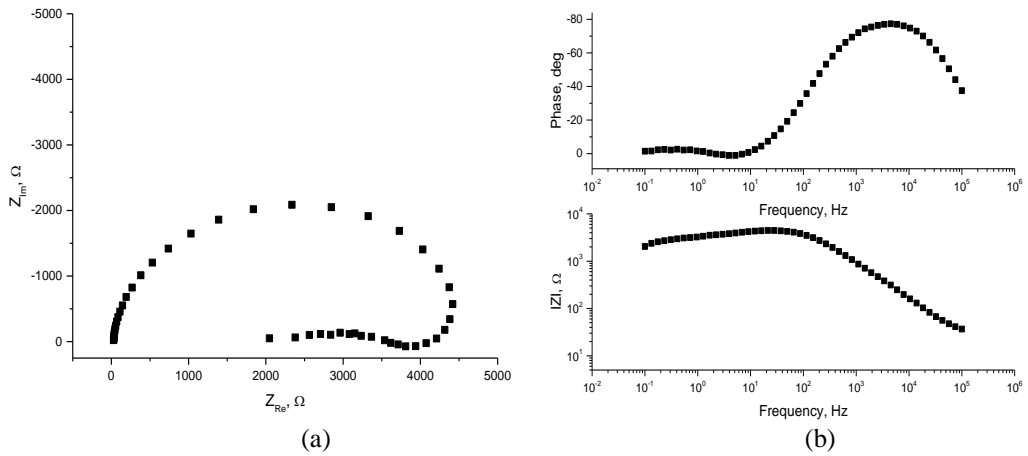


Fig. 8 Nyquist (a) and Bode (b) spectra on Au electrode for  $1 \text{ mM}$  MSG +  $0.5 \text{ M}$   $\text{NaNO}_3$  solution

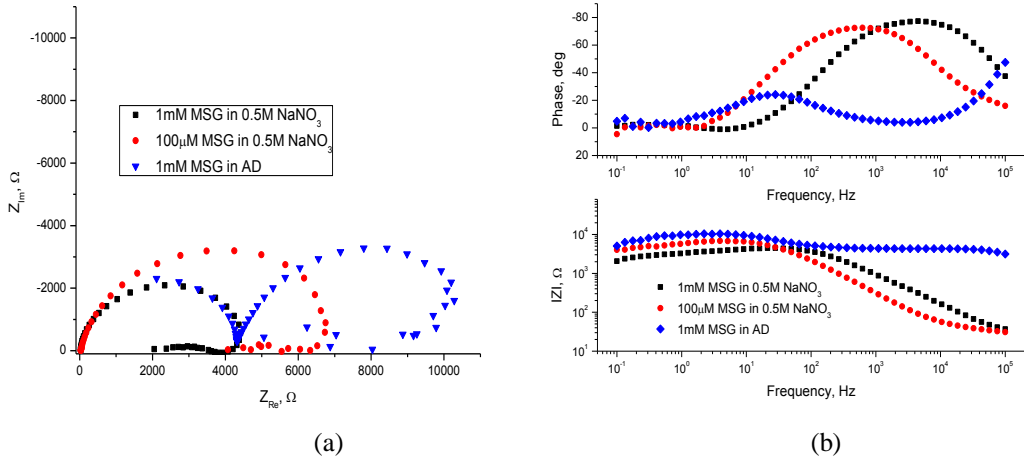


Fig. 9 Comparative Nyquist (a) and Bode (b) on Au electrode for 100  $\mu$ M and 1 mM MSG concentrations without support (in AD) and with 0.5 M  $\text{NaNO}_3$  supporting electrolyte

Fig. 9 presents comparatively Nyquist and Bode spectra on gold SPEs for systems with 0.5 M  $\text{NaNO}_3$  support; spectra for the simple solution 1 mM MSG (dissolved in pure water) are also included. A clear increase in charge transfer by  $\text{NaNO}_3$  addition is seen from Fig. 9a because semicircle of 1 mM MSG + 0.5 M  $\text{NaNO}_3$  has much smaller diameter than of 1 mM MSG simple solution. However, compared to system with  $\text{KNO}_3$  support the  $R_{\text{ct}}$  seems to be much higher in 1 mM MSG + 0.5 M  $\text{NaNO}_3$ , meaning that the exchange current density in electrochemical process is much lower. Also, Bode-angle plots and Bode impedance modulus plots are similar for 100  $\mu$ M and 1 mM MSG in the presence of  $\text{NaNO}_3$  support (Fig. 9b) unlike the systems with  $\text{KNO}_3$ .

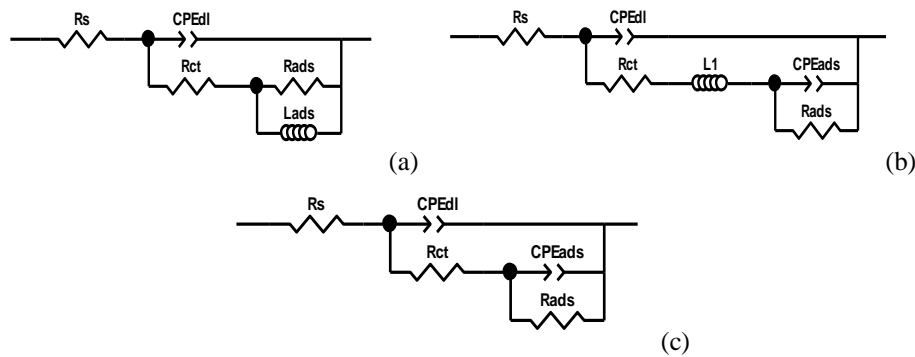


Fig. 10 Equivalent-circuit models of the electrode in the presence of adsorption

The EIS spectra are modelled by equivalent electrical circuits shown in Fig. 10 to fit the obtained impedance data. As can be seen,  $R_s$  resistor is connected in series with a parallel circuit. The parallel scheme comprises different

contributions depending on frequency range: at high frequency the elements are  $R_{ct}$  in parallel with the double layer capacitance (expressed as constant phase element  $CPE_{dl}$ ); the second contribution is related to intermediate and low frequencies where the circuit components are the adsorption resistance ( $R_{ads}$ ), adsorption inductance (noted either  $L_{ads}$  or  $L_1$ ) and adsorption capacitance ( $CPE_{ads}$ ).

We mention that the impedance  $Z$  of a constant CPE is given by:

$$Z_{CPE} = \frac{1}{T(j\omega)^P} \quad (1)$$

where  $T$  is a constant,  $j = \sqrt{-1}$ ,  $\omega$  is angular *ac* frequency and  $P$  is an exponent with values  $0 < P < 1$ . The case  $P=1$  recovers a perfect capacitor. Actually,  $L_{ads}$  is a pseudo-inductance that simulate the situation when the adsorption layer is not constant under cyclic changes in the low frequency potential (see Figs. 1 and 4, for instance); it is related to the presence of a slow adsorption stage unlike a stable adsorption process that occurs in Fig. 5a as an inductive loop. The resulting values of all components from equivalent circuits are given in Table 2.

**Table 2**  
**Fitting results of impedance spectra on gold SPEs for MSG solutions without (AD)/with nitrate salts as supporting electrolyte**

Solution	$R_s$ , $\Omega$	$CPE_{dl}T$ , $\mu F.s^{P-1}$	$CPE_{dl}P$	$R_{ct}$ , $\Omega$	$R_{ads}$ , $\Omega$	$L_{ads}$ or $L_1$ , $\Omega.s$	$CPE_{ads}T$ , $\mu F.s^{P-1}$	$CPE_{ads}P$
100 $\mu M$ MSG in AD <sup>(1)</sup>	23640	7.36	0.84	35092	550000	$3 \times 10^{-11}$	-	-
1 mM MSG in AD <sup>(1)</sup>	4230	2.72	0.86	8036	1557	$8.6 \times 10^{-13}$	-	-
100 $\mu M$ MSG + 0.5 M $KNO_3$ <sup>(1)</sup>	6.6	2.52	0.85	57834	55100	97.67	-	-
1 mM MSG + 0.5 M $KNO_3$ <sup>(2)</sup>	1.8	28.40	0.49	407	$2 \times 10^{-7}$	0.35	14600	0.14
100 $\mu M$ MSG + 0.5 M $NaNO_3$ <sup>(3)</sup>	34.2	1.46	0.88	5113	180	-	1969	0.14
1 mM MSG + 0.5 M $NaNO_3$ <sup>(3)</sup>	~1	0.60	0.85	3153	1500	-	15000	0.13

<sup>(1)</sup>Equivalent circuit from Fig. 10a

<sup>(2)</sup>Equivalent circuit from Fig. 10b

<sup>(3)</sup>Equivalent circuit from Fig. 10c

It can be seen that the fitted data for  $R_s$  and  $R_{ct}$  listed in Table 2 agree well with those experimentally obtained, thus confirming that the addition of supporting electrolyte has led to improvements in ionic conduction and electron transfer rate. Values of  $R_s$  in solution with supporting electrolyte are of the same order of magnitude, whereas the lowest  $R_{ct}$  was determined for 1 mM MSG + 0.5

M KNO<sub>3</sub> solution. Taking into account the surface area of gold screen-printed electrode (0.1256 cm<sup>2</sup>) the fitted values of double layer capacity (expressed by the CPE-T) of several tens of microfarads are plausible, being of usual order of magnitude (35  $\mu$ F cm<sup>-2</sup>) in aqueous solutions. In fact, the exponent P is close to 1 in almost all MSG solutions, meaning a double layer behaving almost like an ideal capacitor. Values of adsorption parameters (resistance, inductance and capacitance) are relatively scattered, illustrating the existence of the adsorption process even if in some cases it is a weak adsorption. In fact, this behavior is also indicated by the values of the exponent CPE<sub>ads</sub>P which is very far from 1.

### 3. Conclusions

Study of the ionic conduction in aqueous solutions of 100  $\mu$ M and 1 mM MSG as well as the charge transfer rate on the gold screen-printed electrode in these solutions was successfully performed by impedance spectroscopy. The addition of either KNO<sub>3</sub> or NaNO<sub>3</sub> as a support electrolyte in a 0.5 M concentration has been shown to significantly improve electrical conduction of MSG solution by about three orders of magnitude. In the same way there was a favorable change in the electron transfer rate expressed by decreasing the R<sub>ct</sub> resistance. Both Nyquist and Bode spectra exhibited a capacitive behavior accompanied by a weak adsorption due to accumulation of different neutral or ionic species from solution. The increase of the MSG concentration illustrated the decrease of the transfer resistance and therefore the increase of exchange current density of the glutamate species in electrochemical processes, as well as the competition for their adsorption with nitrate ions. All impedance parameter changes were highlighted by the fitted data using equivalent electrical circuits as models.

### Acknowledgements

The authors are grateful for the financial support from the National Institute for Laser, Plasma & Radiation Physics (INFLPR) as part of the research project PN-II-RU-TE-2014-4-0976.

### R E F E R E N C E S

- [1]. *I.S. Kucherenko, O. O. Soldatkin, D.Y. Kucherenko, O.V. Soldatkina, S.V. Dzyadevych*, Advances in nanomaterial application in enzyme-based electrochemical biosensors: a review, *Nanoscale Adv.*, **vol. 1**, 2019, pp. 4560-4577.
- [2]. *F.C.O.L. Martins, M.A. Sentanin, D. De Souza*, Analytical methods in food additives determination: Compounds with functional applications, *Food Chem.*, **vol. 272**, 2019, pp. 732-750.
- [3]. *J. Schultz, Z. Uddin, G. Singh, M.M.R. Howlader*, Glutamate sensing in biofluids: recent advances and research challenges of electrochemical sensors, *Analyst*, **vol. 145, no. 2**, 2020, pp. 321-347.
- [4]. *M.G.F. Sales, C. Martins, M.F. Barroso, M.C.V.F. Vaz, M.P.B. Oliveira, C. Delerue-Matos*, Electrochemical evaluations of glutamate at a gold electrode, *Portugaliae Electrochimica Acta*, **vol. 25**, 2007, pp. 173-183.

[5]. *E.V. Dorozhko, E.I. Korotkova, A.A. Shabaeva, A.Y. Mosolkov*, Electrochemical determination of L-glutamate on a carbon-containing electrode modified with gold by voltammetry, *Procedia Chemistry*, **vol. 15**, 2015, pp. 365–370.

[6]. *M. Jamal, S. Chakrabarty, M.A. Yousuf, A. Khosla, K.M. Razeeb*, Micro and nanostructure based electrochemical sensor platform for glutamate detection, *Microsyst. Technol.*, **vol. 24**, no. 10, 2018, pp. 4193-4206.

[7]. *M. Jamal, S. Chakrabarty, H. Shao, D. McNulty, M.A. Yousuf, H. Furukawa, A. Khosla, K.M. Razeeb*, A non enzymatic glutamate sensor based on nickel oxide nanoparticle, *Microsyst. Technol.*, **vol. 24**, no. 10, 2018, pp. 4217–4223.

[8]. *G. Hughes, R.M. Pemberton, P.R. Fielden, J.P. Hart*, Development of a disposable screen printed amperometric biosensor based on glutamate dehydrogenase, for the determination of glutamate in clinical and food applications, *Anal. Bioanal. Electrochem.*, **vol. 6**, no. 4, 2014, pp. 435-449.

[9]. *G. Hughes, R.M. Pemberton, P.R. Fielden, J.P. Hart*, Development of a novel reagentless, screen-printed amperometric biosensor based on glutamate dehydrogenase and NAD<sup>+</sup>, integrated with multi-walled carbon nanotubes for the determination of glutamate in food and clinical applications, *Sens. Actuators B*, **vol. 216**, 2015, pp. 614-621.

[10]. *D. Jiang, Z. Chu, J. Peng, W. Jin*, Screen-printed biosensor chips with Prussian blue nanocubes for the detection of physiological analytes, *Sensors and Actuators B*, **vol. 228**, 2016, pp. 679-687.

[11]. *G. Pioggia, F. Di Francesco, A. Marchetti, M. Ferro, A. Ahluwalia*, A composite sensor array impedimetric electronic tongue: Part I. Characterization, *Biosens. Bioelectron.*, **vol. 22**, no. 11, 2007, pp. 2618-2623.

[12]. *G. Pioggia, F. Di Francesco, M. Ferro, F. Sorrentino, P. Salvo, A. Ahluwalia*, Characterization of a carbon nanotube polymer composite sensor for an impedimetric electronic tongue, *Microchimica Acta*, **vol. 163**, no. 1-2, 2008, pp. 57–62.

[13]. *C.E. Borato, A. Riul, M. Ferreira, O.N. Oliveira, L.H.C. Mattoso*, Exploiting the versatility of taste sensors based on impedance spectroscopy, *Instrum. Sci. Technol.*, **vol. 32**, 2004, pp. 21-30.

[14]. *D. Bajenaru-Georgescu, D. Ionita, M. Prodana, I. Demetrescu*, Electrochemical and antibacterial characterization of thermally treated titanium biomaterials, *UPB Sci. Bull., Series B*, **vol. 77**, no. 4, 2015, pp. 63-74.

[15]. *F. Golgovici, F.G. Ionascu*, Electrochemical behavior of NiCr based alloys in human and artificial saliva, *UPB Sci. Bull., Series B*, **vol. 79**, no. 4, 2017, pp. 157-166.

[16]. *M. Pop, L. Anicai, M. Cristea, M. Ungureanu, M. Enachescu*, Impedance studies on chemically modified electrodes based on 5-[(azulen-1-yl) methylene] ]-2-thioxothiazolidin-4-one, *UPB Sci. Bull., Series B*, **vol. 79**, no. 2, 2017, pp. 3-12.

[17]. *Z. Pahom, F. Branzoi, G. Nechifor*, Electrochemical behaviour of new polymer composite coatings on carbon steel in acid medium, *UPB Sci. Bull., Series B*, **vol. 80**, no. 3, 2018, pp. 117-136.

[18]. [http://www.dropsens.com/en/screen\\_printed\\_electrodes\\_pag.html](http://www.dropsens.com/en/screen_printed_electrodes_pag.html).

[19]. *A.C.F. Ribeiro, M.M. Rodrigo, M.C.F. Barros, L.M.P. Verissimo, C. Romero, A.J.M. Valente, M.A. Esteso*, Mutual diffusion coefficients of L-glutamic acid and monosodium L-glutamate in aqueous solutions at T = 298.15 K, *J. Chem. Thermodynamics*, 74, 2014, 133-137.

[20]. *A. Apelblat, E. Manzurola, Z. Orehkova*, Electrical conductance studies in aqueous solutions with glutamic ions, *Journal of Solution Chemistry*, **vol. 37**, 2007, pp. 891-900.

[21]. *R.C. Weast (Ed.)*, *CRC Handbook of Chemistry, and Physics*, 70th Edition, CRC Press, Boca Raton, FL, 1989, pp. D-221.

[22]. *G.J. Janz, B.G. Oliver, G.I. Lakshminarayanan, G.E. Maye*, Electrical conductance, diffusion, viscosity, and density of sodium nitrate, sodium perchlorate, and sodium thiocyanate in concentrated aqueous solutions, *J. Phys. Chem.*, **vol. 74**, no. 6, 1970, pp. 1285-1289.

[23]. *E.M. Kartzmark*, Conductances, densities, and viscosities of solutions of sodium nitrate in water and in dioxane-water, at 25 °C, *Canadian Journal of Chemistry*, **vol. 50**, 1972, pp. 2845-2850.

[24]. *A.D. Zapata-Lori, M.A. Pech-Canul*, Corrosion inhibition of aluminum in 0.1 m HCl solution by glutamic acid, *Chem. Eng. Comm.*, **vol. 201**, 2014, pp. 855–869.

[25]. *W.A. Badawy, K.M. Ismail, A.M. Fathi*, Corrosion control of Cu–Ni alloys in neutral chloride solutions by amino acids, *Electrochim. Acta*, **vol. 51**, no. 20, 2006, pp. 4182–4189.